ACS Biomaterials SCIENCE & ENGINEERING

pubs.acs.org/journal/abseba

Article

Microneedles with Tunable Dissolution Rate

Himanshu Kathuria, Dennis Lim, Junyu Cai, Bong Geun Chung, and Lifeng Kang*

Cite This: https://dx.doi.org/10.1021/acsbiomaterials.0c00759

Read Online

ACCESS | Metrics & More | Article Recommendations | Supporting Information

ABSTRACT: Dissolvable microneedle (MN) patches have been widely investigated for transdermal drug delivery. The dissolution rate of MN controls the status of drug release from the MN, which in turn determines drug absorption through skin. However, no systematic approaches have been reported to tune the dissolution profile of dissolvable MN matrices. This is the first study to show polyvinylpyrrolidone (PVP)-based dissolvable MN patches with varying dissolution profiles when PVP is copolymerized with cellulose materials. The MN patches were fabricated through thermal curing and photolithography in tandem. The various grades of pharmaceutical cellulose, such as hydroxypropyl methylcellulose and methyl cellulose, have been investigated as dissolution modifier incorporated in the MN patches. The resultant MN patches had dissolution profiles ranging from 45 min to 48 h. The dissolution rates varied with the grades of cellulose materials. Besides dissolution examination, the MN patches were characterized for their mechanical strength, moisture absorption, and skin penetration efficiency. All of the MN patches were able to penetrate the human skin in vitro. Overall, the PVP MN patches have great potential for skin applications as drug carriers with tunable dissolution profiles.

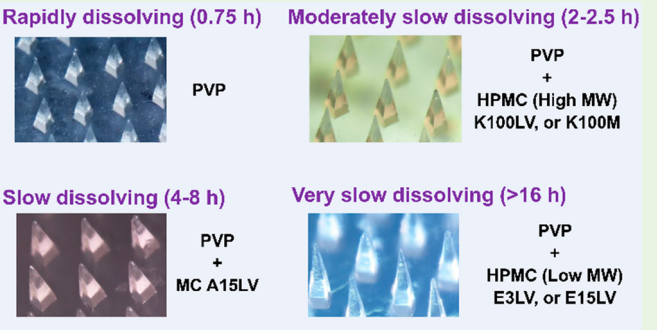

KEYWORDS: *cellulose, polyvinylpyrrolidone, microneedle, dissolution, micromolding, photolithography*

1. INTRODUCTION

The microneedle (MN) has been utilized for local and systemic applications in various disease conditions, such as pain, dermatitis, alopecia, atopic diseases, diabetes, and influenza.[1] Each disease condition requires a distinct delivery strategy, such as immediate or sustained delivery. For instance, the tetanus vaccination requires immediate skin delivery in a single dose, while immunotherapy involves the exposure of an immunotherapeutic agent at progressively increasing dose.[2] Hence, the characteristics of an ideal MN delivery system vary with the need of therapies, skin conditions, and target of delivery.[3]

Compared with hypodermal injections, a dissolving MN patch is more appealing as it is painless, generates no sharp waste, and avoids gastrointestinal adverse reactions. Polyvinylpyrrolidone (PVP) has been widely used as a pharmaceutical and food ingredient. The PVP MN patch for transdermal delivery using various fabrication methods, such as micromolding[4,5] and photolithography,[6,7] has been reported previously. However, the rapid dissolving nature of PVP MNs limits its applications. For instance, the immediate delivery in some disease conditions, such as peanut immunotherapy for peanut allergy, could lead to potential local irritation or systemic anaphylactic reactions caused by rapid exposure of loaded allergens vaccine.[8] Therefore, MN patches with suitable dissolution rates are necessary for such disease conditions.

However, dissolvable MN patches with controlled dissolution profiles remain largely unexplored. Sullvian et al. reported a photolithography approach to form slow-dissolving PVP MN when copolymerized with methacrylic acid.[9] Machekposhti et al. also reported slow-dissolving PVP MN with methacrylic acid copolymerization.[7] Wang et al. reported sustained release of antibodies from nanoparticles loaded into MN.[10] However, the release rate is controlled by loading drugs in nanoparticles rather than in the MN matrix. Hong et al. summarized the various strategies for sustained delivery with dissolvable and biodegradable MN patches.[3] In most cases of dissolvable MN patches, the sustained delivery is achieved using microparticles, nanoparticles, and passive diffusion from backing layers rather than base matrix itself. The use of particulate systems and/or backing layers may potentially increase the complexity of the MN fabrication process and poses as an obstacle for mass production.

To this end, it is preferable if the MN matrix itself has a tunable dissolution profile. Recently, Shakya et al. has shown the peanut immunotherapy using peanut protein coated on

Received: May 20, 2020
Accepted: August 6, 2020
Published: August 6, 2020

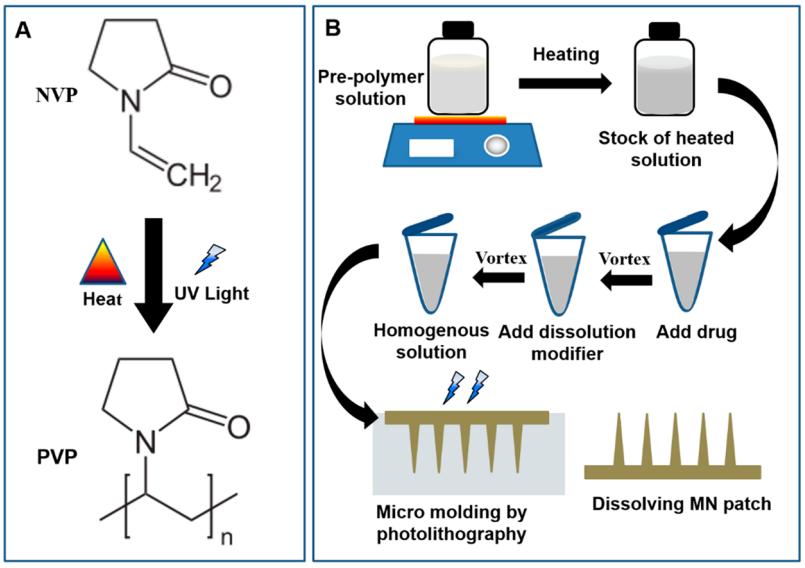

Figure 1. Schematic representation of the (A) polymerization of *N*-vinyl-pyrrolidone into PVP and (B) preparation of the thermopolymerized homogeneous solution and fabrication of the MN patch.

stainless steel MN, where coating and controlled delivery were achieved with the use of carboxymethyl cellulose.[11] Celluloses are widely used in both pharmaceutical and food products. As hydrogels, they can be used to thicken the bulk mixture to prolong drug release. We hypothesize that cellulose materials, such as hydroxypropyl methyl cellulose (HPMC) and methyl cellulose (MC), are useful to control MN dissolution.

In this study, we fabricated the dissolvable PVP MN patch with the incorporation of dissolution modifiers, mainly cellulose materials of various molecular weights. Subsequently, the MN patches were investigated for their functional parameters, such as mechanical strength, moisture absorption, dissolution, and penetration efficiency into skin membranes. A unique method of fabrication was used that allowed the polymerization in a two-step process, i.e., preheating and ultraviolet (UV) light exposure.[12] Through optimization of preheating and UV light exposure, the MN fabrication with modifiers was faster than existing methods, which is another effort toward MN mass production.

2. MATERIALS AND METHODS

2.1. Materials. *N*-Vinylpyrrolidone, 4,4′-azobis (4-cyanovaleric acid) (ABCV), methacrylic acid (MAA), carboxymethyl cellulose sodium (CMC Na), gelatin, and Tofacitinib citrate (TOF) were purchased from Sigma-Aldrich (St. Louis, MO, USA). Hydroxypropyl methylcellulose (HPMC), methylcellulose (MC), and ethyl cellulose (EC) were provided as samples from Colorcon Asia Pacific (Singapore). Peanut protein was purchased from Stallergenes Greer (Lenoir, NC, USA). All materials were used as supplied.

2.2. Fabrication of MN Patches and Loading. *N*-Vinyl-pyrrolidone was mixed with ABCV (100:1 w/w) in an amber bottle and subsequently heated at 90 °C for 12 min (for a 10 mL mixture) (Figure 1). The resultant heated prepolymer solution was cooled, and each modifier was added to form a homogeneous mixture. Subsequently, the homogeneous mixtures were filled into poly-dimethylsiloxane (PDMS) micromolds lubricated with oil and were placed in a vacuum chamber at 90 kPa for 20 min to remove air from the MN channels. The PDMS was fabricated, as previously described[12] and also reported in the Supporting Information (SI1). UV irradiation was performed using a UV lamp (OmniCure S2000) for 30 min before gently being removed from the micromolds (Figure 1B). The UV power and time to cure were optimized to control the texture of MN patches (SI2). As model therapeutics, 1% w/v peanut protein and 1% w/v TOF were also loaded into MN of the dissolvable MN patch to further investigate the effect of the MN properties. TOF was chosen as the model drug, while peanut protein was chosen as the allergen, where both are immunotherapeutic agents.

2.3. Incorporation of Dissolution Modifiers. The common pharmaceutical-grade excipients which have been known to delay drug release in conventional dosage form were tested. The different types of biocompatible cellulose and MAA were selected as potential modifiers to study the delay in dissolution and its application in fabricating dissolvable PVP MN (Table 1).

Table 1. Dissolution Modifiers for PVP MN Patch

dissolution modifier	grade	composition
CMC Na		PVP with CMC Na
ethyl cellulose	S10, S20	PVP with EC
HPMC	E3LV, E15LV, K100LV, K100M	PVP with HPMC
methyl cellulose	A15LV	PVP with MC
MAA		PVP with MAA
gelatin		PVP with gelatin

There were two prerequisites for successful microfabrication. First, the modifier should be miscible with the prepolymer solution to form a homogeneous solution. Next, the homogeneous solution must have enough fluidity to ease filling of micromolds for MN patch fabrication. Investigation of the miscibility was performed by incorporating 1% w/v of an individual modifier into 1 mL of prepolymer solution. The mixture was vortexed for 10 min and was left to stand for 15 min (Figure 1B). The rheological properties of the homogeneous solution depended on the concentration of modifier incorporated. Each modifier was added at progressively increasing concentration into the prepolymer solution to determine the maximum concentration that could keep adequate fluidity for filling the micromold.

To study the dissolution behavior of the materials, a 4 mm hole was punctured in PDMS sheets using a biopsy punch (SI3). This formed a mold for fabricating solid discs of equal volume of the mixtures (Table 1). Afterward, the solid discs were gently removed after being subjected to UV curing. The discs were tested for dissolution in 10 mL of distilled water in a beaker with continuous magnetic stirring.

2.4. Dissolution of MN Patches. Dissolution of MN was tested in a saturated moisture chamber (SI4) at room temperature. First, the

https://dx.doi.org/10.1021/acsbiomaterials.0c00759
ACS Biomater. Sci. Eng. XXXX, XXX, XXX−XXX

chamber was saturated with moisture overnight. The dissolvable MN patch was fixed on the glass slide using double-sided tape and was placed slanted inside a prefabricated PDMS fixture. The PDMS fixture together with dissolvable MN patch was kept in a closed chamber with statured moisture for observation under a stereomicroscope (Nikon SMZ25, Japan). The dissolution process was recorded with the microscope.

2.5. Moisture Absorption. The PVP is hygroscopic, which could affect the functionality of MN patches under storage conditions. In addition, it can also affect the dissolution profile of MNs. Therefore, the MN patches were tested for moisture absorption. The moisture absorption rate was investigated under two different conditions. In first the condition, the MN patches were kept at laboratory conditions (20 °C). In the second condition, the MN patches were placed in a chamber with saturated moisture (SI4). The weight change of the MN patches, caused by moisture absorption, was recorded at various time intervals.

2.6. Mechanical Strength, Penetration Efficiency, and Assay. The mechanical strength of MN was tested using a strain gauge (JSV H1000, JISC., Japan). The MN patches were individually placed on the stage of the strain gauge and were compressed at a compression speed of 20 μm/min up to a load limit of 90 N. The force displacement curve was plotted for all MN patches. In addition, the area under the curve (AUC) was calculated using eq 1. The AUC was calculated up to a displacement of 0.3 mm

$$\text{area under curve (AUC)} = \sum (X_2 - X_1)(Y_1 + Y_2)/2 \quad (1)$$

where X is an independent variable, i.e., displacement (μm), and Y is a dependent variable, i.e., force (N), corresponding to displacement.

The skin penetration ability of MN patches was measured using parafilm[13,14] and human cadaver skin. Briefly, for the parafilm model, the 8 layers of folded parafilm were placed on a PDMS support with a MN patch on the top parafilm layer. The MN patch was pressed using the strain gauge at a speed of 20 mm/min until a force of 25 N was exerted and held for 1 min. Afterward, the number of penetrated holes in each parafilm layer was counted using the stereomicroscope. Further analysis was performed using human cadaver skin samples (Science Care, Phoenix, AZ, USA). The use of cadaver human skin for this study was approved by the National University of Singapore Institutional Review Board. The cadaver skin came from a 92-year-old Caucasian female. Frozen skin samples were thawed at room temperature and cut into 4 cm × 4 cm pieces. The skin pieces were placed on wet tissues to equilibrate for 15 min. The MN patch was applied using the strain gauge with a force of 25 N for 1 min.[15] Afterward, the treated skin was flooded with trypan blue dye for 30 min, the excess dye was removed, and the skin was wiped with 70% ethanol and tissue wipes. The stained micropunctures were recorded under the stereomicroscope.

The amount of TOF encapsulated inside the MN patch was analyzed using a high-performance liquid chromatography (HPLC) method as reported previously.[16] The TOF-loaded MN patches were dissolved in water purified using Millipore Direct-Q prior to the HPLC assay.

3. RESULTS AND DISCUSSION

3.1. Selection of Materials for MN Patch Fabrication. The preliminary studies narrowed the list of potential modifiers. The modifiers of CMC Na, EC, and gelatin did not form a homogeneous solution when mixed with the prepolymer solution. Instead, a suspension was formed with these polymers, which settled down inside the micromold upon application of a vacuum, leading to a phase separation and hence was not amenable for fabrication of the MN patch (Table 2). In contrast, HPMC, MC, and MAA formed homogeneous solutions with the prepolymer solution and were further investigated to fabricate into the MN patches (Table 3).

Table 2. Dissolution Modifiers Not Amenable for Further Investigations

dissolution modifier	concentration	reason
CMC Na	all concentration	form a suspension
EC (S10 and S20)	all concentration	form a suspension
gelatin	all concentration	form a suspension
HPMC (E3LV, E15LV, K100LV, K100M)	10% w/v	too viscous to fill molds
MC A15LV	10% w/v	too viscous to fill molds

Table 3. Dissolution Modifiers Amenable for Further Investigation[a]

modifier	substitution[17]	MW (kDa)	MN dissolution time (h)
HPMC E3LV	hydroxy propyl (7−12%), methoxy (28−30%)	10[18]	∼16 h
HPMC E15LV	hydroxy propyl (7−12%), methoxy (28−30%)	13[18]	>24 h
HPMC K100LV	hydroxy propyl (7−12%), methoxy (19−24%)	25[19]	∼2.5 h
HPMC K100M	hydroxy propyl (7−12%), methoxy (19−24%)	140,[18] 250[19]	∼2 h
MC A15LV	methoxy (27.5−31.5%)	42[20]	∼4 h

[a]The concentration of the modifier in vinylpyrrolidone (VP) is 5% (w/v).

Concerning the rheology, we observed that a 5% w/v of HPMC (all grades) and MC could be incorporated into a prepolymer solution while retaining enough fluidity to fill the micromold. The 10% w/v of HPMC (all grades) and MC were viscous forming a gel-like mixture, which was difficult to fill into microcavities. MAA is liquid, which did not affect the viscosity of the homogeneous solution in a concentration-dependent manner, and we selected a concentration of 20% v/v for further investigations as it allowed easy mixing with the prepolymer solution.

The various modifiers incorporated into the MN patches varied in physical characteristics, which resulted in varying degrees of dissolution delay of the MN patches. The dissolution time of various materials were studied using solid discs made of these materials (SI5). The HPMC caused a delay in dissolution in the following order: E15LV > E3LV > K100LV > K100M. This increasing trend for the various grades of HPMC was found at both concentrations of the modifiers, i.e., 5% w/v and 10% w/v. Incorporation of 5% w/v MC A15LV caused a dissolution delay of 3.8 times more than that of the blank PVP. A further increase in dissolution time (compared to 5% w/v) was observed when the concentration of the various grades of HPMC and MC were increased to 10% w/v. HPMC and MC may form a viscous gel that slows down the diffusion of water molecules required for dissolution to take place.

Across the grades of HPMC from E3LV, E15LV, K100LV, and K100M, the HPMC with a lower MW is associated with greater dissolution delay they conferred (Table 3). The higher methoxy-substituted cellulose (E-grade HPMC) showed slower dissolution compared to lower methoxy-substituted cellulose (K-grade HPMC). MAA, on the other hand, has been proposed to form chemical bonds with PVP, leading to the dissolution delay. Furthermore, incorporation of modifiers

https://dx.doi.org/10.1021/acsbiomaterials.0c00759
ACS Biomater. Sci. Eng. XXXX, XXX, XXX−XXX

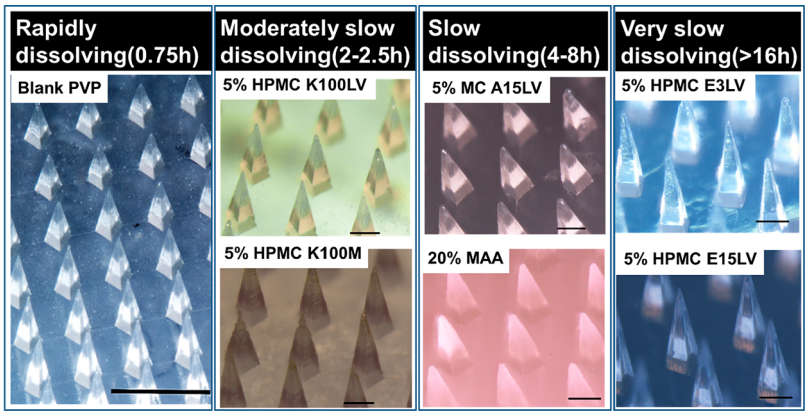

Figure 2. Stereomicroscopic images of dissolving MN patch consisting of various compositions, where rapidly dissolving MN contains PVP, moderately slow dissolving MN contains PVP and 5% HPMC K100LV (or 5% HPMC K100M), slow dissolving MN contains PVP and 5% MC A15LV (or 20% MAA), and very slow dissolving contains PVP and 5% HPMC E15LV (or 5% HPMC E3LV). Base width of the MN is 200 μm. Scale bar for blank PVP MN patch is 1000 and 250 μm for all other MN patches.

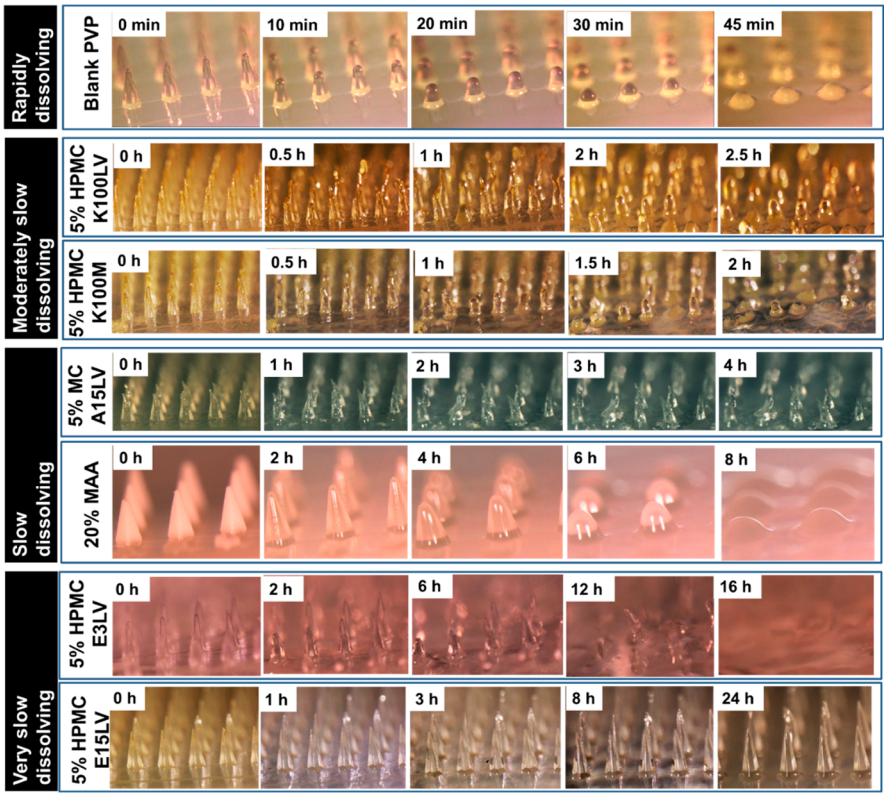

Figure 3. Dissolution of MN patches shown as a microscopic time-lapse image in saturated moisture conditions at room temperature. MN patches with and without modifiers showed different dissolution behavior. Base diameter of the MN is 200 μm.

caused dissolution delay in a concentration-dependent manner. This finding offers a method to alter the concentration of modifiers to fabricate slow-dissolving MN with required dissolution profiles.

3.2. Physical Characteristics of PVP MN Patches. The dimensions of MNs were similar, and the main observable differences among the MN patches were their color and opacity as shown in Figure 2.

3.3. Categorization of Dissolvable MN Patches Based on Dissolution Time. Investigation of the dissolution delay of the MN patches was more complex due to the extensive surface area of the MN, which limited the methods of testing. The observation of MN patches under a microscope upon submerging into distilled water or phosphate buffer saline was not clearly discernible. As a result, we were unable to track the differential dissolution profiles under the stereomicroscope. In addition, submerging the MN patch in water is not an ideal approach for dissolution study, where artificially high water exposure would not mimic the skin conditions, leading to instant dissolution of dissolvable MN patches. In contrast, when investigated under saturated moisture condition, the differences in dissolution times among the MN of various compositions can be clearly visualized (Figure 3 and Videos S1−S4). More importantly, the testing inside saturated vapor would be closer to skin conditions, where the penetrated MN will be dissolved in the interstitial fluid of skin matrix rather

https://dx.doi.org/10.1021/acsbiomaterials.0c00759
ACS Biomater. Sci. Eng. XXXX, XXX, XXX−XXX

than bulk water. Therefore, dissolution testing in saturated vapor was performed. Subsequently, the MN patches were categorized into 4 types based on their dissolution time (Table 4).

Table 4. Categorization of PVP MN Patch with Dissolution Modifiers Based on Dissolution Time Recorded under Saturated Moisture Chamber

dissolution category	dissolution time	dissolution modifier
rapidly dissolving	45 min	none
moderately slow dissolving	2−2.5 h	HPMC K100LV, HPMC K100M
slow dissolving	4−8 h	MC A15LV, MAA
very slow dissolving	>16 h	HPMC E3LV, HPMC E15LV

3.4. Moisture Absorption. It was noteworthy that the MN patches were hygroscopic and had to be stored in desiccators. The absorption of moisture caused the MN patch to become flaccid, which could compromise its mechanical strength. In addition, the absorption of moisture may lead to instability of moisture-sensitive drugs. When exposed in the laboratory environment, the blank PVP MN patch absorbed up to 18% weight of moisture while dissolving MN with modifiers gained about 14−16% weight (Figure 4A). On the other hand, exposure to saturated vapor led to amplified differences in moisture absorption between pure PVP MN patch and MN patches with modifiers (Figure 4B). While the former gained 37% extra weight, the latter absorbed amounts ranging from 17% to 27%.

Under both conditions, the MN patches with modifiers gained less weight than the blank PVP MN patch. This may be attributed to low hydrophilicity of tested modifiers as compared to PVP, leading to slow moisture absorption. Therefore, dissolving MN with the modifiers may be more stable as compared to blank PVP MN patches.

3.5. Mechanical Strength, Penetration Efficiency, and Assay. The mechanical strength of the MN patch is an important factor to determine the ability of the MN to pierce the barrier layer of the skin. As Sun et al. had shown that blank PVP MN patch possessed enough mechanical strength to penetrate the skin,[21] we had to ensure that the incorporation of modifiers would not compromise the mechanical strength of the MN patches. The mechanical strength of MN was compared by plotting their respective force against displacement curves and AUC (Figure 5).

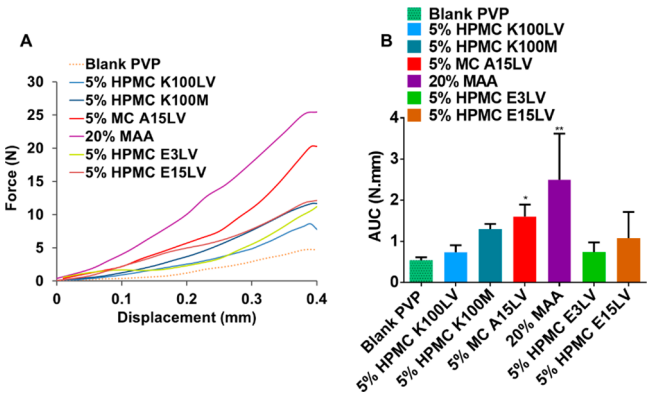

Figure 5. Mechanical properties of PVP MN patches with and without modifiers. (A) Force displacement curve. (B) Area under the curve (AUC) up to displacement of 0.3 mm. Higher AUC shows stronger MN. $*p < 0.05$, $**p < 0.005$.

The resultant curves of the MN patches with modifiers were steeper than that of blank PVP MN patch, showing that greater force could be sustained per unit displacement of compression. Likewise, the higher AUC showed stronger MN. The higher peak strength shown by MNs with modifiers suggested that the MNs were strengthened by addition of the modifiers.

The penetration studies on paraffin film as a model of human skin allowed us to determine the penetration efficiency as well as the depth of penetration, where each layer of the film was measured to be ∼150 μm. The penetration efficiency of all MN patches was above 90% for the first parafilm layer. The MN patches managed a maximum penetration depth of 300 μm in paraffin film, albeit at varying efficiency (Figure 6). The varying penetration efficiency displayed at 300 μm could be due to the bending of MN in the process of being compressed against the paraffin film. We recommend the use of a MN applicator in the future to allow a uniform force distribution among the MN.

Next, the penetration studies done on human cadaver skin samples revealed the differences in penetration efficiency, which could be the consequence of varying degrees of their mechanical strength. Incorporation of MAA resulted in a MN patch with the highest mechanical strength. Simultaneously, dissolving MN with MAA was categorized as "slow dissolving" from the dissolution studies. Therefore, it was consistent that MN with MAA displayed the greatest penetration efficiency in human skin regardless of loading status.

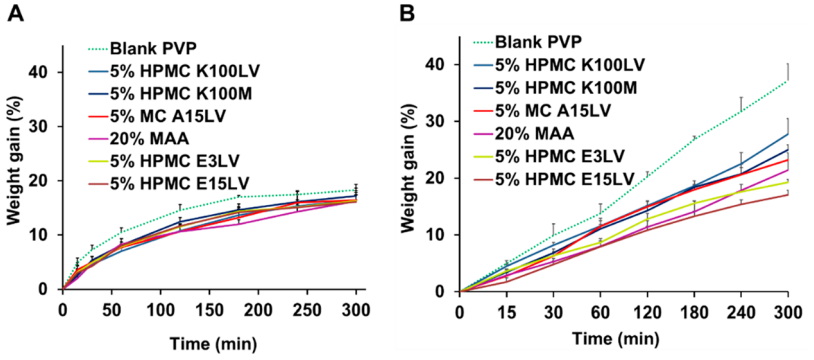

Figure 4. Moisture absorption of dissolving MN patches at room temperature: (A) percent weight gain and (B) percent weight gain in a closed saturated moisture chamber.

https://dx.doi.org/10.1021/acsbiomaterials.0c00759
ACS Biomater. Sci. Eng. XXXX, XXX, XXX−XXX

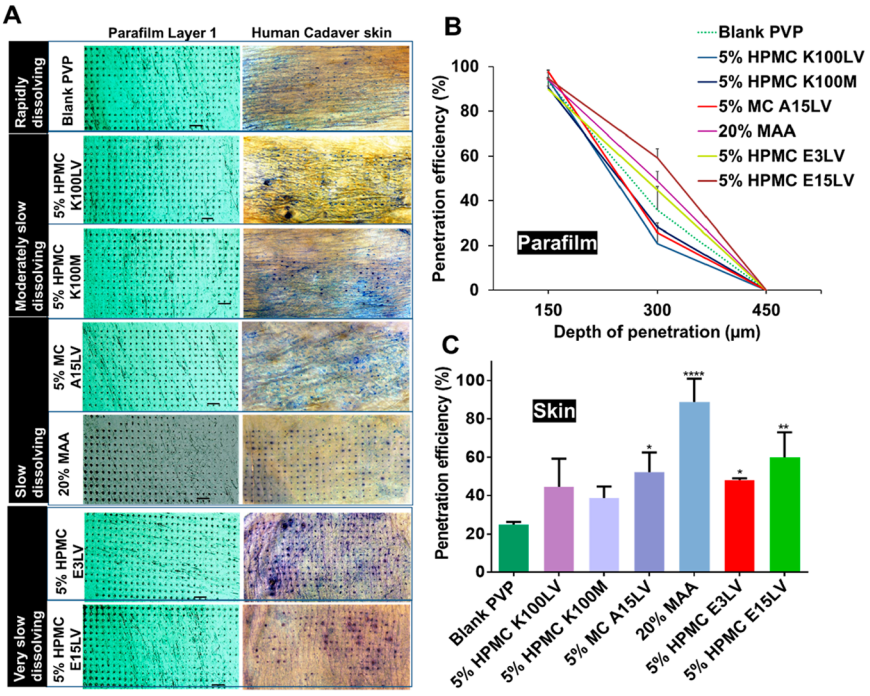

Figure 6. MN penetrations in parafilm and human skin. (A) Microscopic images of micropuntures after MN treatment in parafilm model (layer 1) and human cadaver skin. (B) Percentage penetration of MN patches at different depths in parafilm layers. (C) Percentage penetration of MN patches in human skin. Scale bar = 1000 μm. *p < 0.05, **p < 0.005, ****p< 0.00005.

The skin penetration efficiency depends on the condition of the human cadaver skin, where the skin surface is wet after thawing while the human skin surface is dry. We reduced the surface wetting by use of tissue wipes, but it still inevitably resulted in variability in measurements of the penetration efficiency across MN patches. However, the penetration efficiency was enough for all of the MN patches to penetrate human skin when measured with a widely reported in vitro skin penetration model using parafilm.[13,14,22−25]

Nevertheless, encapsulation of TOF or peanut protein resulted in functional MN as the skin penetration efficiency values remained above that of blank PVP MN, which was taken as our benchmark of a functional MN patch. Skin penetration of TOF and peanut protein-loaded MN patches is shown in SI6.

Finally, the TOF remained stable after fabrication in all MN compositions (SI7). The stability of TOF could be attributed to the method of fabrication, where the use of ABCV, which is a thermal−photo dual-function initiator, allowed TOF to be loaded after partial thermal curing in the fabrication process. As a result, TOF was not exposed to excessive heat. Since the loading of peanut protein was carried out similarly, the benefit of reduced thermal exposure was extended to peanut proteins as well.

3.6. Polymer Safety for MN Applications. PVP less than 20 kDa has been shown to be safely excreted to urine after subcutaneous injection in humans.[9] The PVP in this study is estimated to be ∼5 kDa (SI8), which would be excreted by the kidney in humans.

It has been shown that the subcutaneous injection of HPMC (MW ≈ 29 kDa[26]) was mostly absorbed into the blood and then excreted into the urine and faeces in mice.[27] In this study for the dissolving MN, the cellulose with a low MW, i.e., HPMC E3 LV (MW ≈ 10k), E15 LV (MW ≈ 13k), and HPMC K100 LV (MW ≈ 25k), should be absorbed into systemic circulation and excreted through the kidney. The cellulose with a high MW, i.e., MC A15 LV (MW ≈ 42k) and K100 M (MW ≈ 240k), requires future investigation regarding its excretion. The recent finding of the phagocytosis of HPMC is linked to decomposition of cellulose facilitating excretion, where HPMC with both low and high MW were phagocytized.[27]

In this study, the MN has also been prepared with copolymerization of VP with MAA. Machekposhti et al. performed the toxicity study in rats using MN fabricated with PVP and MAA, which did not show any adverse effects or abnormal changes in mice over 14 days.[7]

4. CONCLUSION

This is the first report to show that dissolution of MN can be tuned with the use of dissolution modifiers, such as pharmaceutical-grade cellulose-based materials. The dissolvable MN patches had enough mechanical strength for skin applications. It can be potentially used as a drug delivery device for different disease conditions requiring controlled drug delivery through the skin.

■ ASSOCIATED CONTENT

Supporting Information

The Supporting Information is available free of charge at https://pubs.acs.org/doi/10.1021/acsbiomaterials.0c00759.

Fabrication of micromold, optimization of photopolymerization, dissolution delay, schematic of the MN dissolution setup, skin penetration of MN loaded with TOF and peanut protein, and HPLC assay of TOF (PDF)

Rapidly dissolving MN contains PVP (AVI)

https://dx.doi.org/10.1021/acsbiomaterials.0c00759
ACS Biomater. Sci. Eng. XXXX, XXX, XXX−XXX

Very slow dissolving MN contains PVP and 5% HPMC E15LV (AVI)

Moderately slow dissolving MN contains PVP and 5% HPMC K100M (AVI)

Slow dissolving MN contains PVP and 20% MAA (AVI)

AUTHOR INFORMATION

Corresponding Author

Lifeng Kang − *School of Pharmacy, Faculty of Medicine and Health, University of Sydney, Sydney, New South Wales 2006, Australia;* orcid.org/0000-0002-1676-7607; Phone: + 61 286276361; Email: lifeng.kang@sydney.edu.au

Authors

Himanshu Kathuria − *Department of Pharmacy, National University of Singapore, Singapore 117543 Singapore*

Dennis Lim − *Department of Pharmacy, National University of Singapore, Singapore 117543 Singapore*

Junyu Cai − *School of Pharmacy, Faculty of Medicine and Health, University of Sydney, Sydney, New South Wales 2006, Australia*

Bong Geun Chung − *Department of Mechanical Engineering, Sogang University, Seoul 04107, Korea;* orcid.org/0000-0002-6838-3218

Complete contact information is available at: https://pubs.acs.org/10.1021/acsbiomaterials.0c00759

Notes

The authors declare no competing financial interest.

ABBREVIATIONS

AUC, area under curve; ABCV, 4,4′-azobis(4-cyanovaleric acid); CMC Na, carboxymethyl cellulose sodium; EC, ethyl cellulose; HPMC E15LV, higher viscosity "E" grade of HPMC; HPMC E3LV, lower viscosity "E" grade of HPMC; HPMC K100LV, lower viscosity "K" grade of HPMC; HPMC K100M, higher viscosity "K" grade of HPMC; HPMC, hydroxypropyl methylcellulose; MAA, methacrylic acid; MC, methylcellulose; MC A15LV, grade of MC; MN, microneedle; PDMS, polydimethylsiloxane; PVP, polyvinylpyrrolidone; TOF, Tofacitinib citrate; UV, ultraviolet

REFERENCES

(1) Kathuria, H.; Kochhar, J. S.; Kang, L. Micro and nanoneedles for drug delivery and biosensing. *Ther. Delivery* **2018**, *9* (7), 489−492.

(2) Hwang, M. P.; Fecek, R. J.; Qin, T.; Storkus, W. J.; Wang, Y. Single injection of IL-12 coacervate as an effective therapy against B16-F10 melanoma in mice. *J. Controlled Release* **2020**, *318*, 270−278.

(3) Yuan, W.; Hong, X.; Wu, Z.; Chen, L.; Liu, Z.; Wu, F.; Liangming Wei, L. Dissolving and biodegradable microneedle technologies for transdermal sustained delivery of drug and vaccine. *Drug Des., Dev. Ther.* **2013**, *7*, 945−952.

(4) Ronnander, P.; Simon, L.; Spilgies, H.; Koch, A.; Scherr, S. Dissolving polyvinylpyrrolidone-based microneedle systems for in-vitro delivery of sumatriptan succinate. *Eur. J. Pharm. Sci.* **2018**, *114*, 84−92.

(5) Koh, K. J.; Liu, Y.; Lim, S. H.; Loh, X. J.; Kang, L.; Lim, C. Y.; Phua, K. K. L. Formulation, characterization and evaluation of mRNA-loaded dissolvable polymeric microneedles (RNApatch). *Sci. Rep.* **2018**, *8* (1), 11842.

(6) Lin, Y. H.; Lee, I. C.; Hsu, W. C.; Hsu, C. H.; Chang, K. P.; Gao, S. S. Rapid fabrication method of a microneedle mold with controllable needle height and width. *Biomed. Microdevices* **2016**, *18* (5), 85.

(7) Machekposhti, S. A.; Soltani, M.; Najafizadeh, P.; Ebrahimi, S. A.; Chen, P. Biocompatible polymer microneedle for topical/dermal delivery of tranexamic acid. *J. Controlled Release* **2017**, *261*, 87−92.

(8) Kowalski, M. L.; Ansotegui, I.; Aberer, W.; Al-Ahmad, M.; Akdis, M.; Ballmer-Weber, B. K.; Beyer, K.; Blanca, M.; Brown, S.; Bunnag, C.; Hulett, A. C.; Castells, M.; Chng, H. H.; De Blay, F.; Ebisawa, M.; Fineman, S.; Golden, D. B.; Haahtela, T.; Kaliner, M.; Katelaris, C.; Lee, B. W.; Makowska, J.; Muller, U.; Mullol, J.; Oppenheimer, J.; Park, H. S.; Parkerson, J.; Passalacqua, G.; Pawankar, R.; Renz, H.; Rueff, F.; Sanchez-Borges, M.; Sastre, J.; Scadding, G.; Sicherer, S.; Tantilipikorn, P.; Tracy, J.; van Kempen, V.; Bohle, B.; Canonica, G. W.; Caraballo, L.; Gomez, M.; Ito, K.; Jensen-Jarolim, E.; Larche, M.; Melioli, G.; Poulsen, L. K.; Valenta, R.; Zuberbier, T. Risk and safety requirements for diagnostic and therapeutic procedures in allergology: World Allergy Organization Statement. *World Allergy Organ. J.* **2016**, *9* (1), 33.

(9) Sullivan, S. P.; Murthy, N.; Prausnitz, M. R. Minimally invasive protein delivery with rapidly dissolving polymer microneedles. *Adv. Mater.* **2008**, *20* (5), 933−938.

(10) Wang, C.; Ye, Y.; Hochu, G. M.; Sadeghifar, H.; Gu, Z. Enhanced cancer immunotherapy by microneedle patch-assisted delivery of anti-PD1 antibody. *Nano Lett.* **2016**, *16* (4), 2334−40.

(11) Shakya, A. K.; Ingrole, R. S. J.; Joshi, G.; Uddin, M. J.; Anvari, S.; Davis, C. M.; Gill, H. S. Microneedles coated with peanut allergen enable desensitization of peanut sensitized mice. *J. Controlled Release* **2019**, *314*, 38−47.

(12) Kathuria, H.; Kang, K.; Cai, J.; Kang, L. Rapid microneedle fabrication by heating and photolithography. *Int. J. Pharm.* **2020**, *575*, 118992.

(13) Larraneta, E.; Moore, J.; Vicente-Perez, E. M.; Gonzalez-Vazquez, P.; Lutton, R.; Woolfson, A. D.; Donnelly, R. F. A proposed model membrane and test method for microneedle insertion studies. *Int. J. Pharm.* **2014**, *472* (1−2), 65−73.

(14) Quinn, H. L.; Bonham, L.; Hughes, C. M.; Donnelly, R. F. Design of a dissolving microneedle platform for transdermal delivery of a fixed-dose combination of cardiovascular drugs. *J. Pharm. Sci.* **2015**, *104* (10), 3490−500.

(15) Kathuria, H.; Fong, M. H.; Kang, L. Fabrication of photomasks consisting microlenses for the production of polymeric microneedle array. *Drug Delivery Transl. Res.* **2015**, *5* (4), 438−50.

(16) Shankar, V. K.; Dhiman, V.; Giri, K. K.; Sharma, K.; Zainuddin, M.; Mullangi, R. Development and validation of a RP-HPLC method for the quantitation of tofacitinib in rat plasma and its application to a pharmacokinetic study. *Biomed. Chromatogr.* **2015**, *29* (9), 1325−1329.

(17) Dow Chemistry of methocel cellulose ethers: a technical review; https://msdssearch.dow.com/PublishedLiteratureDOWCOM/dh_08e5/0901b803808e5f58.pdf?filepath=dowwolff/pdfs/noreg/198-02289.pdf&fromPage=GetDoc (accessed 12/07/2020).

(18) Chavan, R. B.; Thipparaboina, R.; Kumar, D.; Shastri, N. R. Evaluation of the inhibitory potential of HPMC, PVP and HPC polymers on nucleation and crystal growth. *RSC Adv.* **2016**, *6* (81), 77569−77576.

(19) Hiremath, P. S.; Saha, R. N. Controlled release hydrophilic matrix tablet formulations of isoniazid: design and in vitro studies. *AAPS PharmSciTech* **2008**, *9* (4), 1171−8.

(20) Nasatto, P. L.; Pignon, F.; Silveira, J. L. M.; Duarte, M. E. R.; Noseda, M. D.; Rinaudo, M. Interfacial properties of methylcelluloses: the influence of molar mass. *Polymers* **2014**, *6* (12), 2961−2973.

(21) Sun, W.; Araci, Z.; Inayathullah, M.; Manickam, S.; Zhang, X.; Bruce, M. A.; Marinkovich, M. P.; Lane, A. T.; Milla, C.; Rajadas, J.; Butte, M. J. Polyvinylpyrrolidone microneedles enable delivery of intact proteins for diagnostic and therapeutic applications. *Acta Biomater.* **2013**, *9* (8), 7767−74.

(22) Ripolin, A.; Quinn, J.; Larraneta, E.; Vicente-Perez, E. M.; Barry, J.; Donnelly, R. F. Successful application of large microneedle patches by human volunteers. *Int. J. Pharm.* **2017**, *521* (1−2), 92−101.

(23) Caffarel-Salvador, E.; Kearney, M. C.; Mairs, R.; Gallo, L.; Stewart, S. A.; Brady, A. J.; Donnelly, R. F. Methylene blue-loaded dissolving microneedles: potential use in photodynamic antimicrobial chemotherapy of infected wounds. *Pharmaceutics* **2015**, *7* (4), 397−412.
(24) Abdelghany, S.; Tekko, I. A.; Vora, L.; Larraneta, E.; Permana, A. D.; Donnelly, R. F. Nanosuspension-based dissolving microneedle arrays for intradermal delivery of curcumin. *Pharmaceutics* **2019**, *11* (7), 308.
(25) Lhernould, M. S.; Deleers, M.; Delchambre, A. Hollow polymer microneedles array resistance and insertion tests. *Int. J. Pharm.* **2015**, *480* (1−2), 152−7.
(26) Danjo, K.; Kozaki, K.; Sunada, H.; Otsuka, A. Influence of the molecular weight of binding agents on the physical properties of granules and tablets. *Chem. Pharm. Bull.* **1994**, *42* (10), 2121−2125.
(27) Teruya, K.; Oguma, A.; Nishizawa, K.; Kawata, M.; Sakasegawa, Y.; Kamitakahara, H.; Doh-Ura, K. A single subcutaneous injection of cellulose ethers administered long before infection confers sustained protection against prion diseases in rodents. *PLoS Pathog.* **2016**, *12* (12), e1006045.

https://dx.doi.org/10.1021/acsbiomaterials.0c00759
ACS Biomater. Sci. Eng. XXXX, XXX, XXX−XXX